Journal of Sound and Vibration (2001) **243**(3), 503–524
doi:10.1006/jsvi.2000.3421, available online at http://www.idealibrary.com on IDEAL®

MORE DETAILS ABOUT THE INTERACTION OF FORCED AND PARAMETRIC RESONANCES ARISING FROM IN-PLANE EXCITATION OF IMPERFECT RECTANGULAR PLATES

S. Sassi and H. Smaoui

Department of Physics and Instrumentation, Institut National des Sciences Appliquées et de Technologie, Centre Urbain Nord, B.P. 676, 1080 *Tunis Cedex, Tunisie*

AND

M. Thomas and F. Laville

Department of Mechanical Engineering, École de Technologie Supérieure, 1100, *rue Notre-Dame Ouest, Montréal, Québec, Canada H3C 1K3*

(*Received* 2 *September* 1999, *and in final form* 17 *October* 2000)

The goal of the present paper is to improve our understanding of the response of the in-plane loaded rectangular plates containing initial geometric imperfection. Besides the frequency responses and FFT curves, which were used as diagnostic tools in previous investigations, the temporal response and the phase diagram have been added to better study the transition zones between two kinds of vibration modes. The phase portrait shows that the plate response has a number of "unusual and perhaps chaotic" characteristics in the transition from one mechanism of vibration of another, which distinguished it from the more classical periodic response. Moreover, the effect of one particular spatial mode of imperfection on a different mode of vibration has been investigated for the first time. It was found that the maximum amplitude of forced vibrations is large when vibration and imperfection are in the same mode while the first mode of vibration is always excited whatever the mode of imperfection is.

1. INTRODUCTION

In the particular fields of aerospace, aeronautics and transportation, the search for structures that could travel more rapidly, consume less energy and offer better comfort and security, has obliged engineers to use light materials and build thin-walled structures. As the effort to make such structures lighter and thinner is increasing, there is a growing concern among scientists and researchers about the mechanical behavior and reactions of such structures whenever they are exposed to a static or dynamic loading.

In particular, when a plate is subjected to an out-of-plane sinusoidal loading it exhibits a well-known forced resonance. However, when the plate is subjected to in-plane loading, the problem becomes more complicated and the plate response prediction is quite difficult because of the lateral instability (buckling) induced by such in-plane loading. When the in-plane loading is dynamic (for example, of the form $N_{YO} + N_{YT}\cos \Lambda T$), the plate may exhibit a lateral instability over certain regions of the (N_{YO}, N_{YT}, Λ) parameter space and several kinds of vibrations could take place (forced, parametric, etc.) [1]. The studies of Ostiguy and Nguyen [1–3] thoroughly explain the plate behavior whenever it vibrates with

0022-460X/01/230503 + 22 $35.00/0

a parametric mechanism of instability. Such a resonance occurs when the excitation frequency Λ is approximately equal to twice the natural frequency $\Omega_i(\Lambda = 2\Omega_i)$ of the mode number i. The parametric resonance is characterized by a double-sided motion and an abrupt entrance in the instability zone.

In the presence of an initial geometric imperfection (initial lateral deflection under zero inplane loading), the stability problem becomes much more complicated. Indeed, such unavoidable imperfections are found to be responsible for the following:

- The increase of resonance frequencies [4].
- The change of the non-linear vibration behavior from the familiar hard spring to the soft-spring type for small vibration amplitude [5].
- The existence of forced vibrations, which occurs when the excitation frequency Λ is equal to the natural frequency Ω_i ($\Lambda = \Omega_i$). This resonance is also characterized by a one-sided oscillating motion with a small vibration amplitude (compared to parametric resonance) and a gradual entrance into the instability zone [5, 6].

When the forced and parametric vibrations are well separated, the response of the plate can be evaluated without ambiguity. However, when both of them are partially or totally overlapping, the global response of the plate becomes unpredictable. Experimental evidence of simultaneous and combination resonances, due to the interaction of forced and parametric vibrations, presented by Ostiguy [1], Ostiguy *et al.* [3], constitutes an original and significant contribution.

To the best of our knowledge, the first explanation of what could happen if, for a certain excitation frequency, forced and parametric vibrations exist simultaneously, was given by Ostiguy and Sassi using an analytical asymptotic approach [5, 6]. More recently, Sassi *et al.* [7] implemented a direct integration method on a computer to solve numerically the differential equations of motion. In addition to verifying results previously obtained with the asymptotic method, it was possible to go beyond and verify experimental results not modelled with the asymptotic method and bring to light the coalescence phenomenon that had not previously been observed. The simulation results were also used to explain modal interactions between forced–forced, parametric–parametric and forced–parametric resonances.

The recent studies of Ostiguy and St-Georges [8, 9], using also a direct integration method by a second-order Adams–Bashforth integrator, show that only the stable part of the resonance curve can be obtained. They also found that the temporal response obtained for parametric vibrations in non-symmetric relative to the static position of equilibrium. The predominantly "inward" deflection response (as viewed from the center of curvature) of an imperfect plate is confirmed. Moreover, for a structure with a sufficiently large initial imperfection, the well-known hard-spring behavior of the principal parametric resonance curve becomes a soft-spring behavior for small vibration amplitudes. However, for large vibration amplitudes, the curve exhibits the usual hard-spring behavior. This kind of resonance curve is characterized by a jump phenomenon at the beginning of the parametric resonance. The soft-spring behavior is influenced by the size of the imperfection, the vibration mode, the size of the static force, the aspect ratio of the plate and the boundary conditions.

The goal of the present paper is to improve our understanding of the response of the in-plane loaded rectangular plates containing initial geometric imperfection. Emphasis will be put on the study of instabilities in the transition zones between two kinds of vibration modes. To better explain these phenomena, in addition to the frequency responses and FFT curves used in the previous analysis, the temporal response and the phase diagram have been added.

2. CONCEPTUAL MODEL

Because the conceptual model was presented in detail in a previous paper by Sassi *et al.* [7], only the key elements are presented in this paper. The study is performed for a thin rectangular plate of uniform thickness "h" with initial geometric imperfections. The material is elastic, homogenous and isotropic. The plate analyzed is considered to be "stress free" and the edges are free to move in the plane of the perfect undeformed plate. The plate is subjected to the action of in-plane forces uniformly distributed along two opposite edges. The loading is achieved with a static component superposed with a periodic component whose excitation frequency is Λ, as shown in Figure 1.

The temporal differential equations describing the motion of this plate, are expressed as follows [7]:

$$\ddot{W}_m + 2C_m\dot{W}_m + \bar{\Omega}_m^2 W_m - 2\cos\theta \sum_n \mu_m^n \bar{\Omega}_n^2 (W_n + I_n)$$

$$+ \sum_q \sum_r \sum_s M_v^{qrs} W_q W_r W_s + \sum_q \sum_s \sum_l H_v^{qsl} W_q W_s I_l = 0. \tag{1}$$

In the non-dimensional equation (1), μ_m^n represents a loading parameter, C_m is the coefficient of viscous damping, $\bar{\Omega}_m$ is the free vibration frequency of the imperfect rectangular plate loaded by a constant component of the in-plane force, M_v^{qrs} and H_v^{qsl} are the coefficients of the non-linear coupling terms, $I_n = (W_{0n} + d_{0n})$ is the total static deflection, W_{0n} is the initial geometric imperfection, and d_{0n} is the initial deflection caused by the static component of the applied in-plane load.

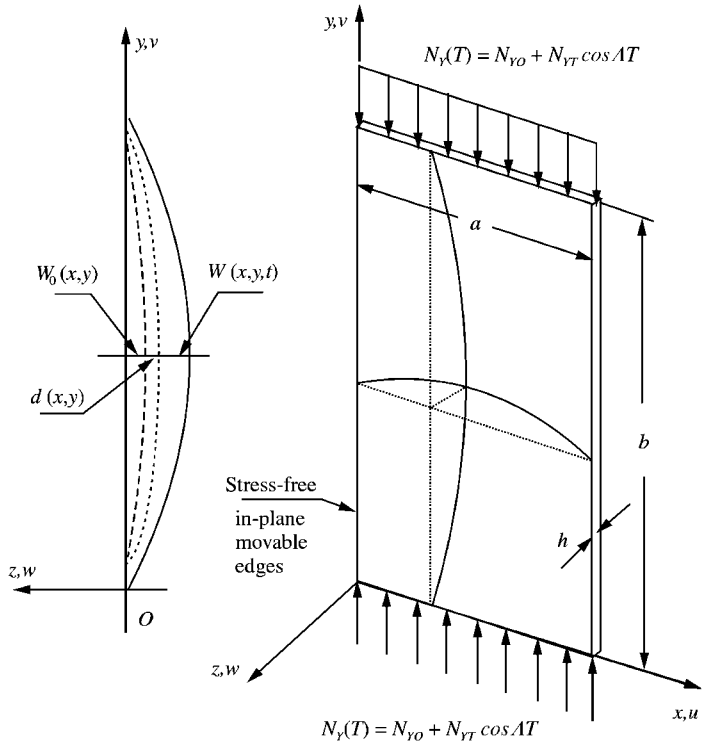

Figure 1. Plate parameters (dimensions, coordinates, boundary conditions and load configuration).

It is obvious that the more the terms that exist in the expansion of the transverse displacement, the more accurate is the solution. However, to keep the resolution manageable, only the first three terms are kept. The continuous system is reduced to a three-degree-of-freedom model.

Moreover, because of the complexity of equation (1) and in order to simplify our investigation, the interaction between the three modes of vibrations will be studied with only two modes at a time (modes i and k) in the presence of only one spatial mode of imperfection (mode k). Therefore

$$W_i \neq 0, \qquad W_{0i} = 0, \qquad W_k \neq 0, \qquad W_{0k} \neq 0. \tag{2}$$

Equation (1) is reduced to the following two equations corresponding respectively to modes i and k:

$$\begin{aligned} \ddot{W}_i + \bar{\Omega}_i^2 W_i + C_i \dot{W}_i - 2\cos\theta \lfloor \mu_i^i \bar{\Omega}_i^2 W_i + \mu_i^k \bar{\Omega}_k^2 (W_k + I_k) \rfloor \\ + [\Gamma_{i1} W_i^3 + \Gamma_{i3} W_i^2 W_k + \Gamma_{i5} W_i W_k^2 + \Gamma_{i9} W_k^3] \\ + [H_i^{iik} W_i^2 + H_i^{ikk} W_i W_k + H_i^{kkk} W_k^2] I_k = 0, \end{aligned} \tag{3}$$

$$\begin{aligned} \ddot{W}_k + \bar{\Omega}_k^2 W_k + 2C_k \dot{W}_k - 2\cos\theta \lfloor \mu_k^i \bar{\Omega}_i^2 W_i + \mu_k^k \bar{\Omega}_k^2 (W_k + I_k) \rfloor \\ + [\Gamma_{k1} W_i^3 + \Gamma_{k3} W_i^2 W_k + \Gamma_{k5} W_i W_k^2 + \Gamma_{k9} W_k^3] \\ + [H_k^{iik} W_i^2 + H_k^{ikk} W_i W_k + H_k^{kkk} W_k^2] I_k = 0, \end{aligned} \tag{4}$$

where Γ_m are non-linear coefficients defined as

$$\Gamma_{m1} = M_m^{iii}, \qquad \Gamma_{m3} = M_m^{iik} + M_m^{iki} + M_m^{kii}, \qquad \Gamma_{m9} = M_m^{kkk}, \qquad \Gamma_{m5} = M_m^{ikk} + M_m^{kik} + M_m^{kki}, \tag{5}$$

This set of non-linear differential equations has been solved by direct numerical integration using the SIMULINK toolbox of MATLAB as thoroughly explained before [7]. However, with this method, only the stable part of the resonance can be obtained, exactly like the physical system, but it gives enough information to predict and understand the behavior of the real physical system.

3. RESULTS AND DISCUSSION

The parameters and material constants of the rectangular plate for which the simulation has been conducted are listed in Table 1. In order to increase gradually the complexity of

TABLE 1

Specifications of plate parameters

Dimensions, $a \times b \times h$ (mm) $= 293 \times 508 \times 1$
Aspect ratio, R $(b/a) = 1{\cdot}734$
Modulus of elasticity, $E = 2{\cdot}385$ GPa
Poisson's ratio, $v = 0{\cdot}45$
Density, $\rho = 1200$ Kg/m^3
Damping, $\Delta = 2\pi C/\bar{\Omega}$

the problem, the plate dynamic response in the presence of initial imperfection is analyzed first in the case of a single mode of vibration. This simpler case is also convenient to illustrate more easily the use of the different graphical outputs to understand the plate response mechanism. This is done for an imperfection in the same mode as the vibration. Then the effect of choosing a different imperfection mode is investigated. Finally, the plate response is modelled using two modes and the results are interpreted in the same way as in the case of the single mode.

3.1. DYNAMIC RESPONSE OF THE PLATE FOR A SINGLE MODE OF VIBRATION

In this part, we have considered that both the vibration and the imperfection are in the same mode, which is mode 1. The imperfection value is $W_0 = (0{\cdot}2, 0, 0)$ and represents "0·2 times the thickness of the plate" in this first mode. The numerical integration graphical outputs in Figure 2 show respectively the global and filtered responses. The forced resonance is located around 9·73 Hz, whereas the parametric resonance is located between 17·40 and 34·26 Hz.

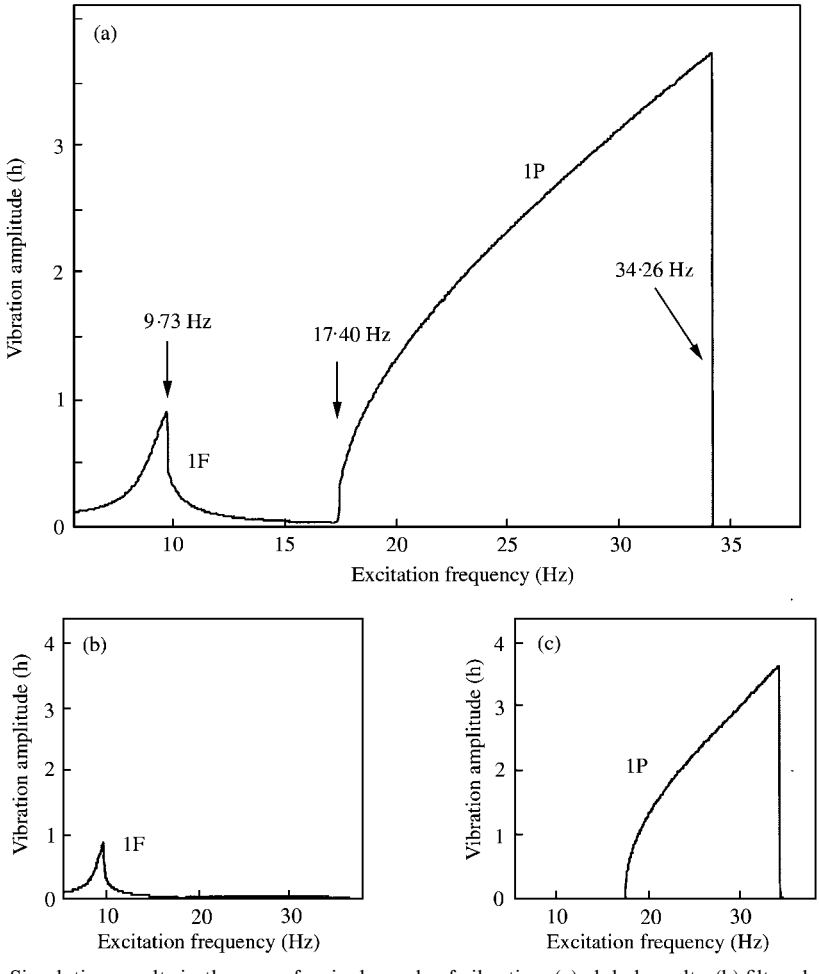

Figure 2. Simulation results in the case of a single mode of vibration; (a) global results; (b) filtered response of mode 1 forced; (c) filtered response of mode 1 parametric. $W_0 = (0{\cdot}2, 0, 0)$, $\Delta = 0{\cdot}2$, $N_{YO} = 0{\cdot}5$, $N_{YT} = 0{\cdot}2$.

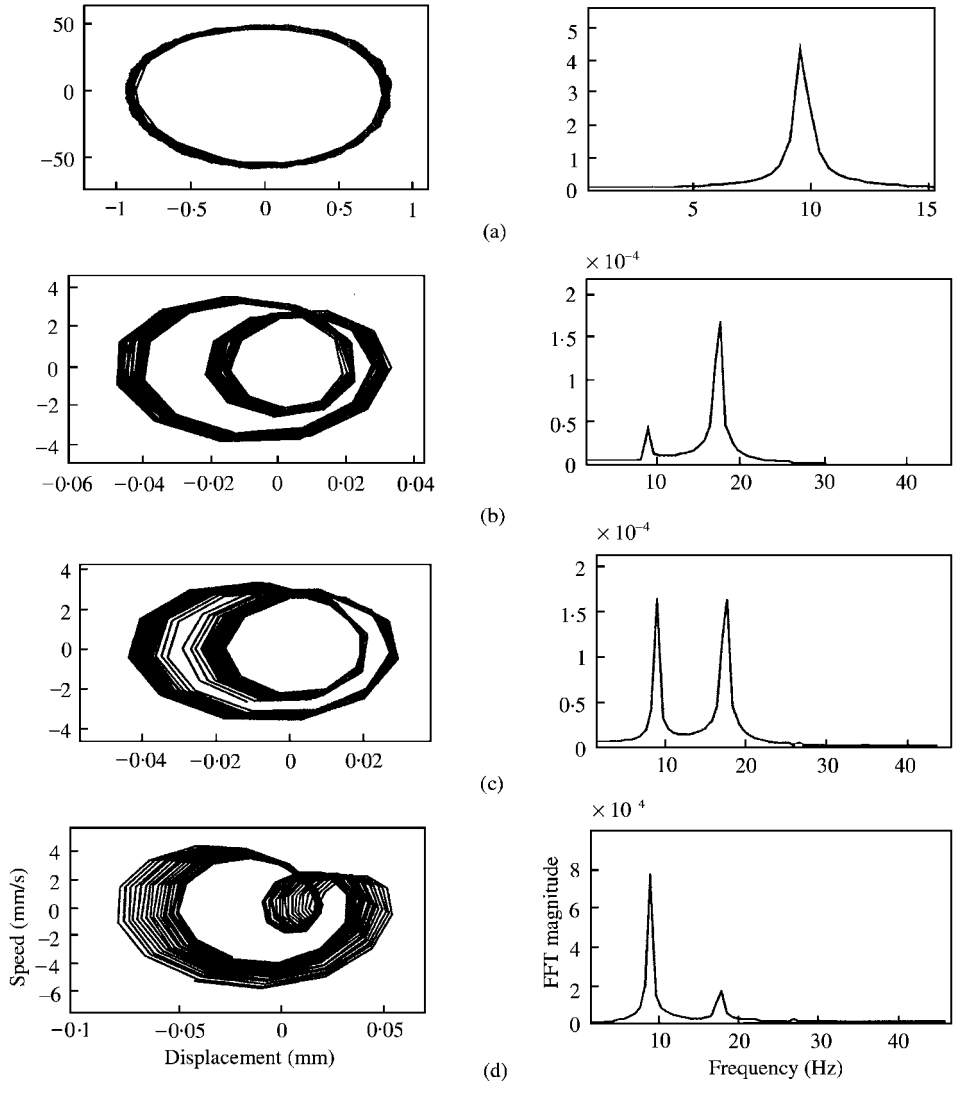

Figure 3. Global simulation results (Phase diagram and FFT) at the excitation frequency of: (a) $\Lambda = 9{\cdot}68$ Hz; (b) $\Lambda = 17{\cdot}22$ Hz; (c) $\Lambda = 17{\cdot}36$ Hz; (d) $\Lambda = 17{\cdot}40$ Hz. $W_0 = (0{\cdot}2, 0, 0)$, $\Delta = 0{\cdot}2$, $N_{YO} = 0{\cdot}5$, $N_{YT} = 0{\cdot}2$.

Figure 3(a) presents phase diagrams, and FFT magnitudes for an excitation frequency ($\Lambda = 9{\cdot}68$ Hz) which is located in the forced zone. The analysis of these figures reveals that, for this case, the plate vibrates purely in the forced regime. Indeed, the FFT curves show that the frequencies of excitation and response are exactly the same. One should note that the amplitude of vibrations [in the frequency response curve of Figure 2(a)] increases in a progressive manner until it reaches a maximum after which it drops suddenly. This limit, localized at 9·73 Hz, corresponds to the end of the forced instability zone (after this limit, forced vibrations continue to exist but their amplitude is small).

Figures 3(b)–4(b) clarify the different responses for some excitation frequencies in the parametric zone and especially the changes of behavior at the entry and at the exist of such a zone. The sequence of FFT magnitude curves shows that the parametric resonance

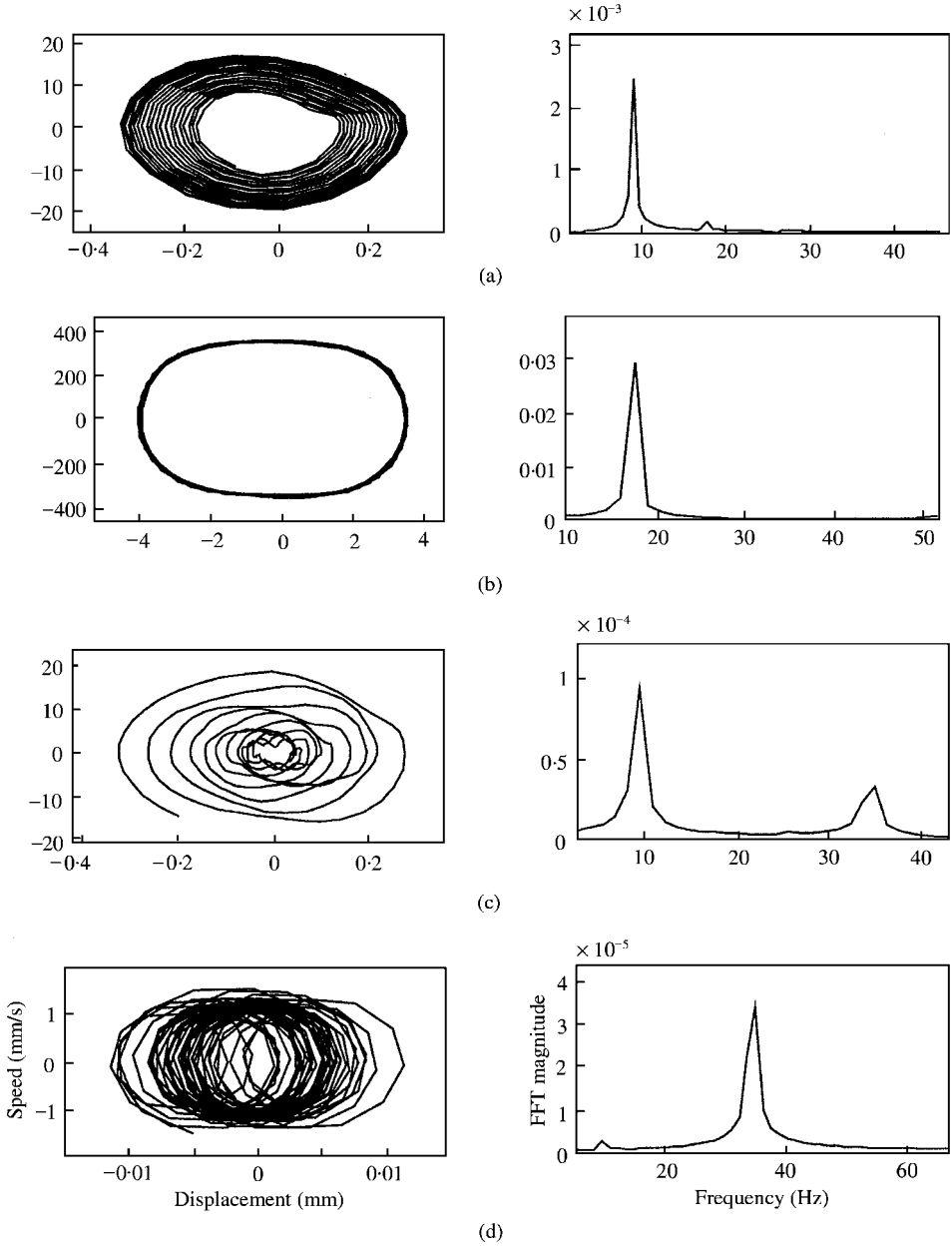

Figure 4. Global simulation results (Phase diagram and FFT) at the excitation frequency of: (a) $\Lambda = 17{\cdot}45$ Hz; (b) $\Lambda = 34{\cdot}17$ Hz; (c) $\Lambda = 34{\cdot}26$ Hz; (d) $\Lambda = 34{\cdot}31$ Hz. $W_0 = (0{\cdot}2, 0, 0)$, $\Delta = 0{\cdot}2$, $N_{YO} = 0{\cdot}5$, $N_{YT} = 0{\cdot}2$.

appears and disappears in a sudden manner and can reach much larger amplitudes than the forced ones. These two principal characteristics of parametric resonance make it a very harmful type of resonance. It should also be noted that, when crossing the entry limit of the parametric zone, there is not only an increase of the movement amplitude but also a switch of the vibration frequency to half of the excitation value.

The entry of the plate in the parametric instability zone is accomplished as follows.

- At 16·50 Hz, the response is forced.

- At 17·22 Hz (Figure 3(b)), the forced-parametric transition has already taken place. The phase diagram presents two major loops. The FFT curve presents two peaks: one at 17·22 Hz of large amplitude and the other at 8·61 Hz of small amplitude, indicating clearly the existence of two periodic movements: a strong forced vibration with the beginning of a parametric vibration.
- As the frequency of excitation increases, the competition between forced and parametric mechanisms favors more this latter one. Indeed, at 17·36 Hz (Figure 3(c)), the FFT curve shows an equal energy distribution between the two peaks. But at 17·40 Hz (Figure 3(d)), the peak at 8·7 Hz dominates the one at 17·40 Hz and the response becomes mainly parametric.

Starting at 17·45 Hz (Figures 4(a) and 4(b), the response is purely parametric and the amplitude of the movement increases considerably. The phase diagram shows an evolution of the circular pattern. There is shrinkage in one direction and expansion in the other. From a practical standpoint, this means that, during a peak-to-peak motion, the acceleration level of the plate is low through the middle position and high toward the extreme positions. The plate will preserve its parametric behavior until the end of the parametric instability zone located at 34·26 Hz, after which there is a sudden drop of the amplitude to a nearly null value. Since it is not prepared beforehand for this change, the plate will pass through a state of dwell, characterized by an irregular shape of the phase diagram, when the excitation is in the vicinity of 34·26 Hz (Figure 4(c)). Above this frequency, the plate regains its "stability" and continues to vibrate with a forced mechanism of very small amplitude (Figure 4(d)).

3.2. EFFECT OF THE IMPERFECTION MODE AND AMPLITUDE ON THE FORCED VIBRATION AMPLITUDE

As already mentioned in previous papers [6, 7], the forced vibration existence is mainly due to the existence of initial geometrical imperfections in the plate and the maximum of amplitude is also related to the imperfection amplitude. However, no information was found about the relationship between the maximum of forced oscillations and the imperfection amplitude, whenever the imperfection and vibration modes are different. To establish this relationship, the present work has considered the case where the imperfection mode is different from the vibration mode. In Figure 5 are plotted the maximum amplitudes of forced vibrations (just before the drop point) for the first three modes against the value of imperfection for one of the three modes. These plots show that the amplitude of forced vibration is particularly large when vibration and imperfection are in the same spatial mode. One can see also that the first mode of vibration is easily excited in the presence of any mode of imperfection. Its amplitude grows rapidly when the imperfection increases. However, things are quite different when the mode of vibration is symmetric and the mode of imperfection is anti-symmetric or *vice versa*. In this case, the imperfection acts against the vibration.

3.3. DYNAMIC RESPONSE OF THE PLATE FOR TWO MODES OF VIBRATION

The numerical simulation of the dynamic behavior of an imperfect rectangular plate modelled with two degrees of freedom (the first and the second spatial modes) is computed and presented in the following section. The plate possesses an initial imperfection of "0·2

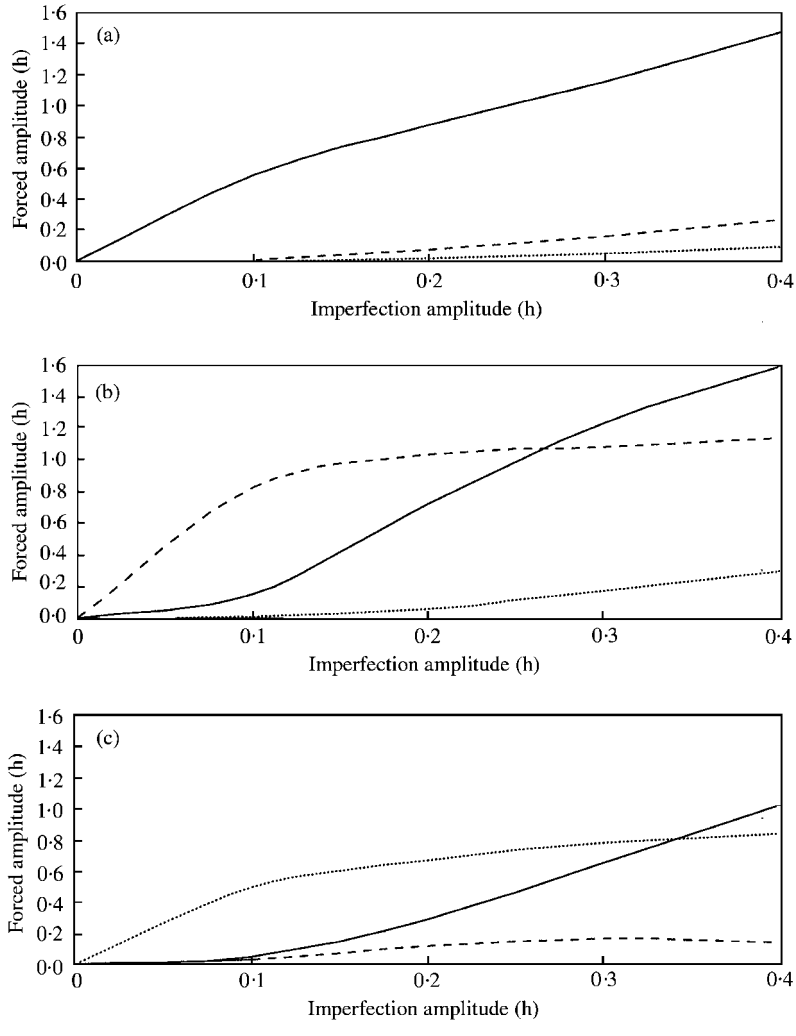

Figure 5. Effect of imperfection on the maximum amplitude of forced vibrations. (a) Mode 1 of imperfection; (b) mode 2 of imperfection; (c) mode 3 of imperfection. ——, Mode 1 of vibration; – – – –, mode 2; · · · · · , mode 3; $\Delta = 0{\cdot}2$, $N_{YO} = 0{\cdot}5$, $N_{YT} = 0{\cdot}2$.

times the plate thickness", first in its first mode (Figures 6 and 7) represented by $W_0 = (0{\cdot}2, 0{\cdot}0, 0{\cdot}0)$, and then in its second mode (Figure 8) represented by $W_0 = (0{\cdot}0, 0{\cdot}2, 0{\cdot}0)$.

For the particular conditions of Figure 6, the two natural frequencies of the first and the second spatial modes are respectively 9·14 and 14·41 Hz. Consequently, one would have to expect theoretically: a forced resonance of the first mode (1F) located around 9·14 Hz, a forced resonance of the second mode (2F) located around 14·41 Hz, a parametric resonance of the first mode (1P) located around 18·28 Hz, and a parametric resonance of the second mode (2P) located around 28·82 Hz. The zones of instability of these different resonance are close to each other and especially the two zones (2F) and (1P) which lead to a possible interaction between them. If each mode is studied separately, the forced resonance (2F) would start at 14·41 Hz and drop before 15 Hz (Figure 7(b)). However, because of the modal interaction, the forced instability zone will be stretched to 18·66 Hz which is an unexpected new limit (Figure 7(a)).

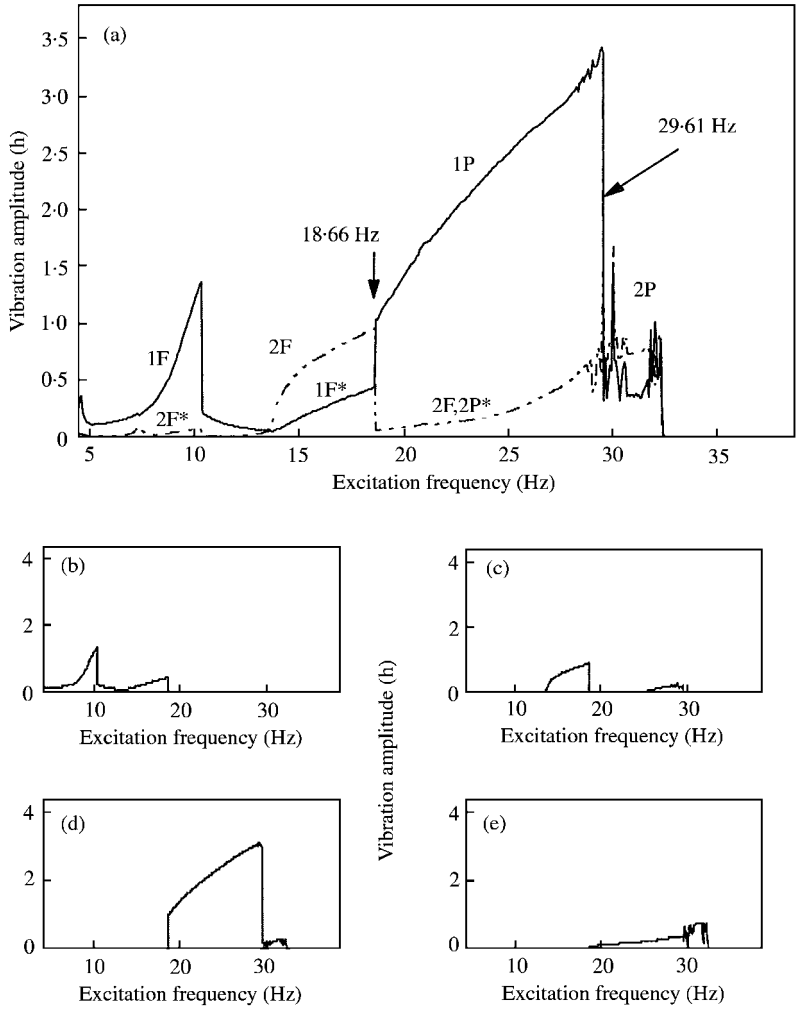

Figure 6. Effect of imperfection of mode 1 on the interaction between forced and parametric modes of vibration. (a) Global response; (b) mode 1 forced; (c) mode 2 forced; (d) mode 1 parametric; (e) mode 2 parametric. $W_0 = (0{\cdot}2, 0, 0)$, $\Delta = 0{\cdot}1$, $N_{YO} = 0{\cdot}5$, $N_{YT} = 0{\cdot}2$.

Figure 9, relative to 15·99 Hz, shows that the two spatial modes of vibrations are excited and both of them show a forced instability mechanism clearly identified by a peak located at the same frequency as the excitation. However, mode 2 is the one that dominates the response. Its amplitude is larger, its behavior is more regular and its phase diagram is more smooth. The full domination of the forced mode (2F), not only excludes the mode (1P) but also indirectly excites the mode (1F). This phenomenon of resonance of different modes with the same frequency is called "coalescence" and is an intrinsic characterization of non-linear problems.

The understanding of the plate vibratory behavior excited at the particular frequency of 18·66 Hz (frequency of transition) is as interesting as the knowledge of its behavior before and after this frequency. The different aspects of the plate response are plotted in Figure 10. At the beginning, the plate exhibits a well-identified hesitation between vibrating in one or

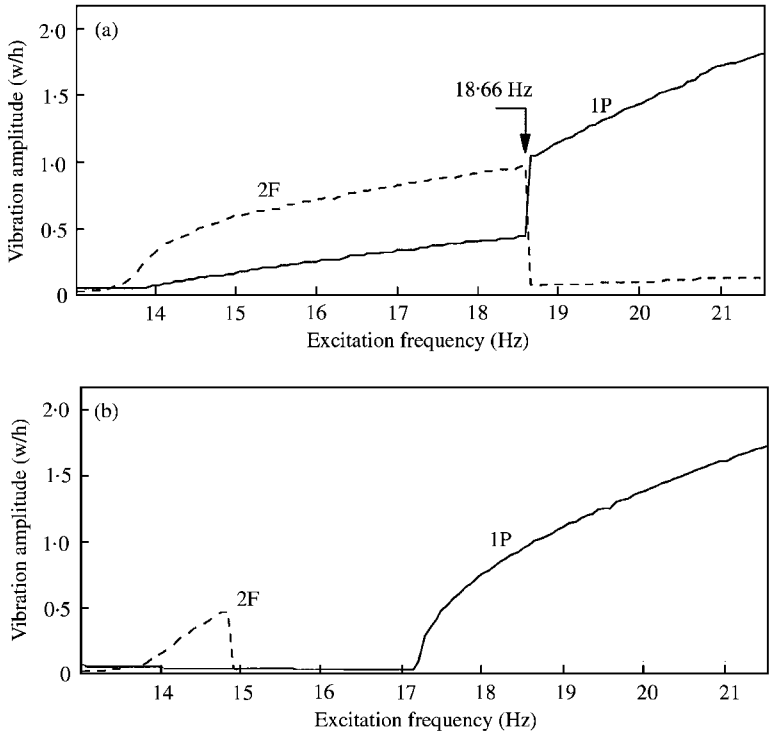

Figure 7. Effect of imperfection of mode 1 on the interaction between forced and parametric modes of vibration. (a) Coupled modes; (b) uncoupled modes. $W_0 = (0{\cdot}2, 0, 0)$, $\Delta = 0{\cdot}1$, $N_{YO} = 0{\cdot}5$, $N_{YT} = 0{\cdot}2$.

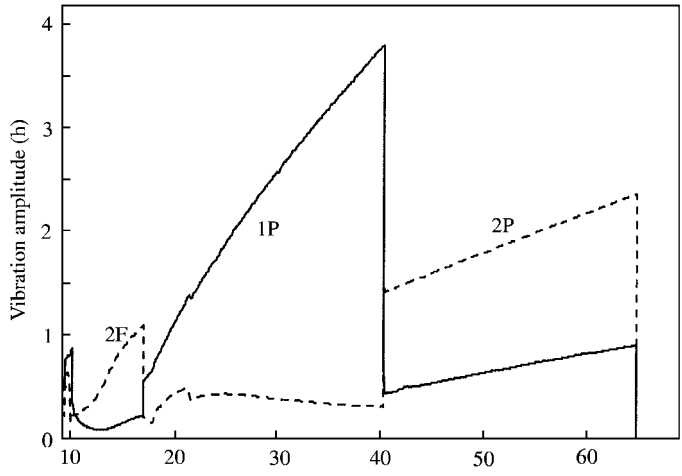

Figure 8. Effect of imperfection of mode 2 on the interaction between forced and parametric modes of vibration. $W_0 = (0, 0{\cdot}2, 0)$, $\Delta = 0{\cdot}1$, $N_{YO} = 0{\cdot}5$, $N_{YT} = 0{\cdot}2$.

the other regimes. Finally, it finishes by converging to a stable state dominated by parametric vibrations. During this transition, a transfer of energy is observed from the forced mode (2F) to the parametric mode (1P) while the vibration amplitude is nearly null.

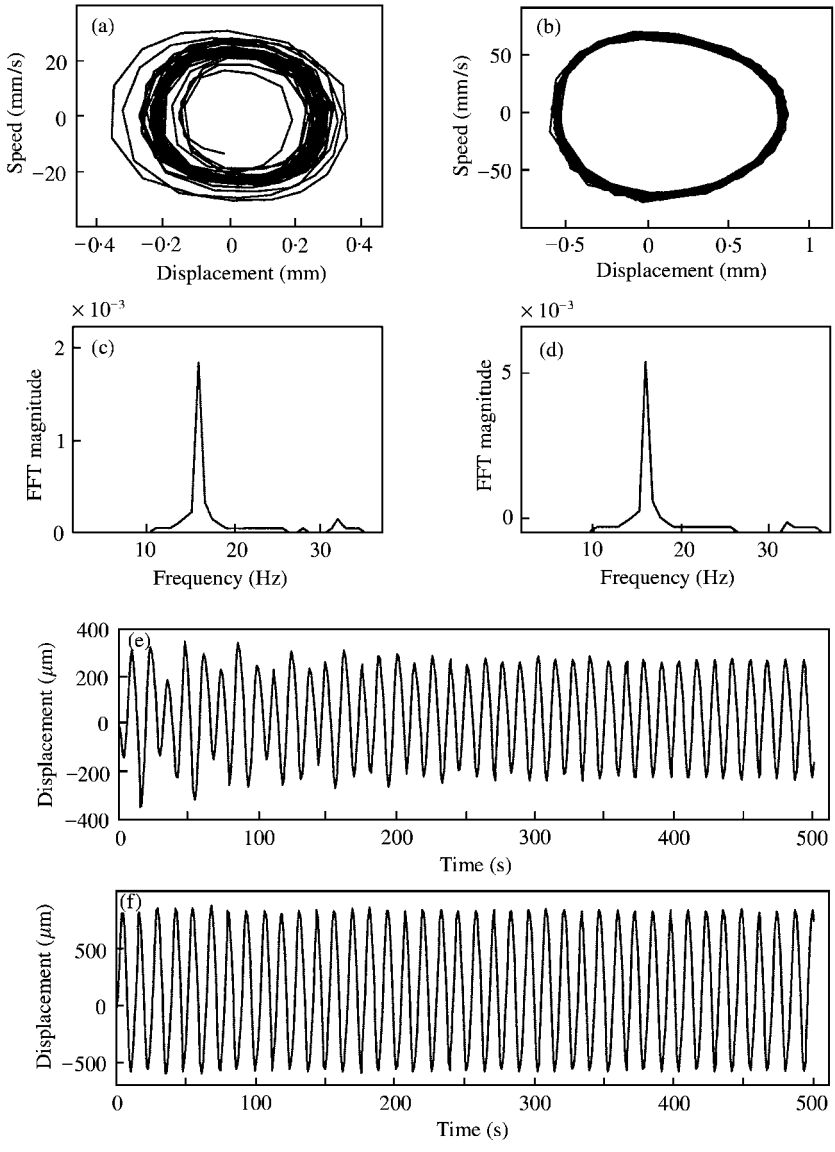

Figure 9. Global simulation results at the frequency excitation of 15·99 Hz. (a) Phase diagram of mode 1; (b) phase diagram of mode 2; (c) FFT of mode 1; (d) FFT of mode 2; (e) temporal response of mode 1; (f) temporal response of mode 2. $W_0 = (0{\cdot}2, 0, 0)$, $\Delta = 0{\cdot}2$, $N_{YO} = 0{\cdot}5$, $N_{YT} = 0{\cdot}2$.

Figure 11 shows the vibratory behavior of the plate for an excitation frequency $\Lambda = 18{\cdot}73$ Hz. For all the frequencies located after 18·66 Hz, one can note that spatial mode 1 oscillates with a purely parametric resonance (1P) while mode 2 oscillates with both forced and parametric resonances (2F) and (2P) but with a net domination of the parametric one. Hence the plate will vibrate at two different frequencies (Λ and $\Lambda/2$) although it is excited at a single frequency (Λ). The forced oscillations of mode 2 (2F) continue to exist with small amplitudes although the region is dominated by parametric vibrations.

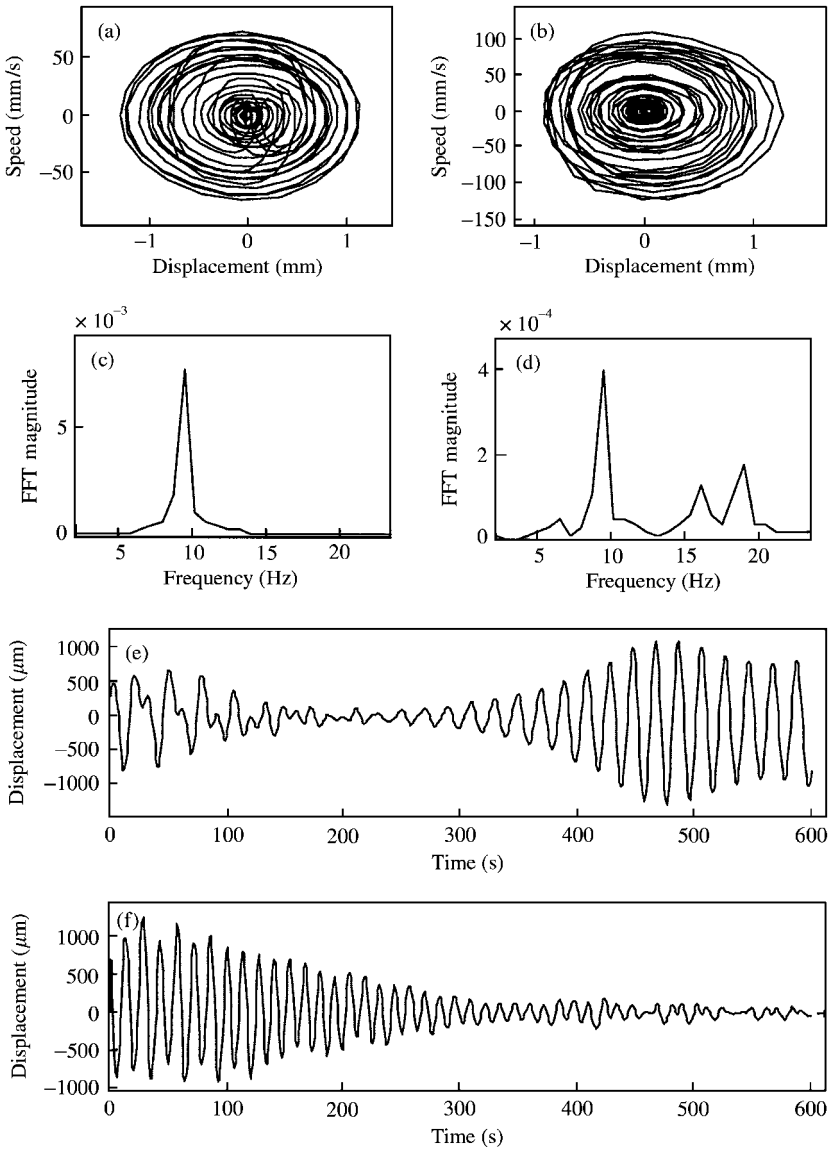

Figure 10. Global simulation results at the frequency excitation of 18·66 Hz. (a) Phase diagram of mode 1; (b) phase diagram of mode 2; (c) FFT of mode 1; (d) FFT of mode 2; (e) temporal response of mode 1; (f) temporal response of mode 2. $W_0 = (0{\cdot}2, 0, 0)$, $\Delta = 0{\cdot}2$, $N_{YO} = 0{\cdot}5$, $N_{YT} = 0{\cdot}2$.

The mode (1P) will dominate the response of the plate until the excitation frequency reaches 28·82 Hz which is the starting point of mode (2P). The modal interaction between the two modes (1P) and (2P) will induce a sudden drop of the amplitude at 29·61 Hz after which an hesitation phenomenon is clearly observed. The sequences of phase diagram and FFT curves taken at different frequencies around this critical value of 29·61 Hz show how sudden was this switch in the response. As indicated in Figures 12 and 13, the phase portrait of mode 2 is quite convoluted and difficult to understand. When the limit of 29·61 Hz is crossed (Figures 13–18), mode 1 is also driven into this agitation. The steady state response of the plate will have a number of "unusual or perhaps chaotic" characteristics which

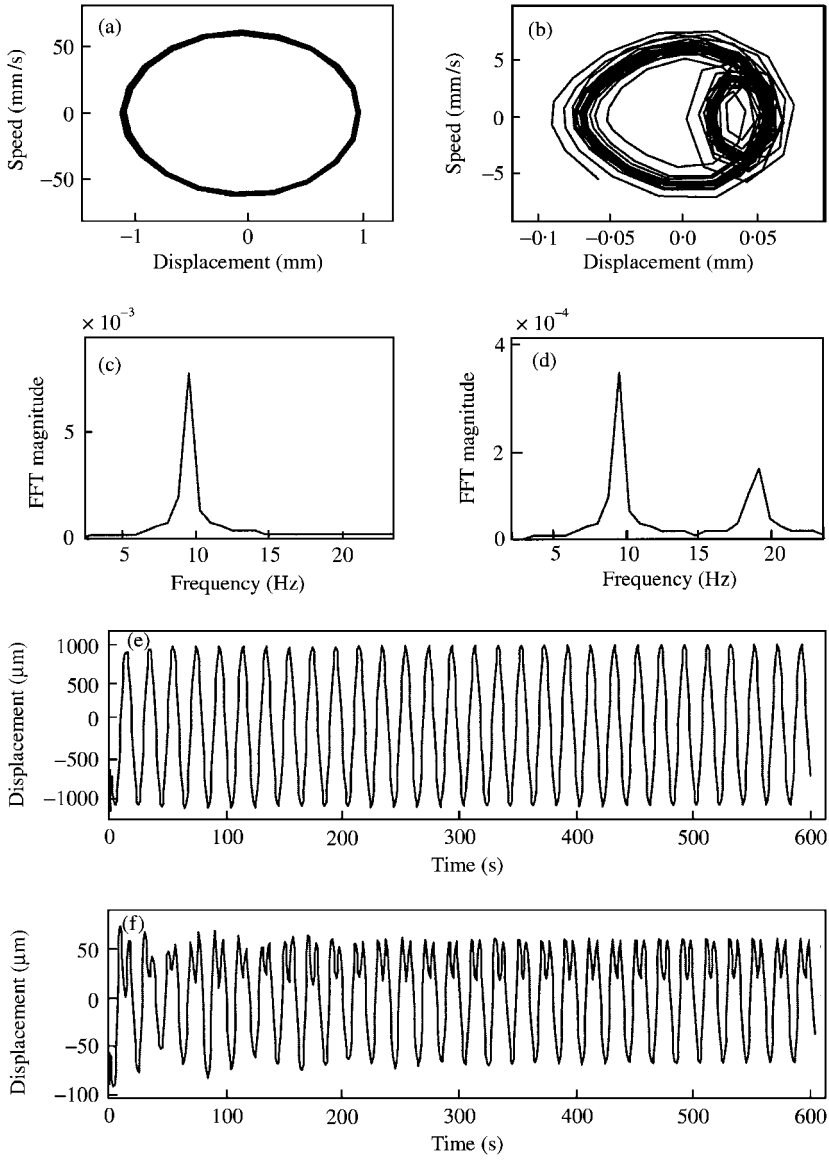

Figure 11. Global simulation results at the frequency excitation of 18·73 Hz. (a) Phase diagram of mode 1; (b) phase diagram of mode 2; (c) FFT of mode 1; (d) FFT of mode 2; (e) temporal response of mode 1; (f) temporal response of mode 2. $W_0 = (0{\cdot}2, 0, 0)$, $\Delta = 0{\cdot}2$, $N_{YO} = 0{\cdot}5$, $N_{YT} = 0{\cdot}2$.

distinguished it from the more classical periodic response. This steady state response has the following characteristics.

- It is aperiodic, never repeating itself, even though the excitation is periodic.
- There is some broadband frequency content, indicating a certain degree of randomness.

Observing again Figure 6, the global frequency response shows that the mode (2P) disappears also after the excitation frequency reaches 34·26 Hz, which is the upper limit of mode 1 parametric instability. On the contrary, Figure 8 shows that the mode (2P) is present

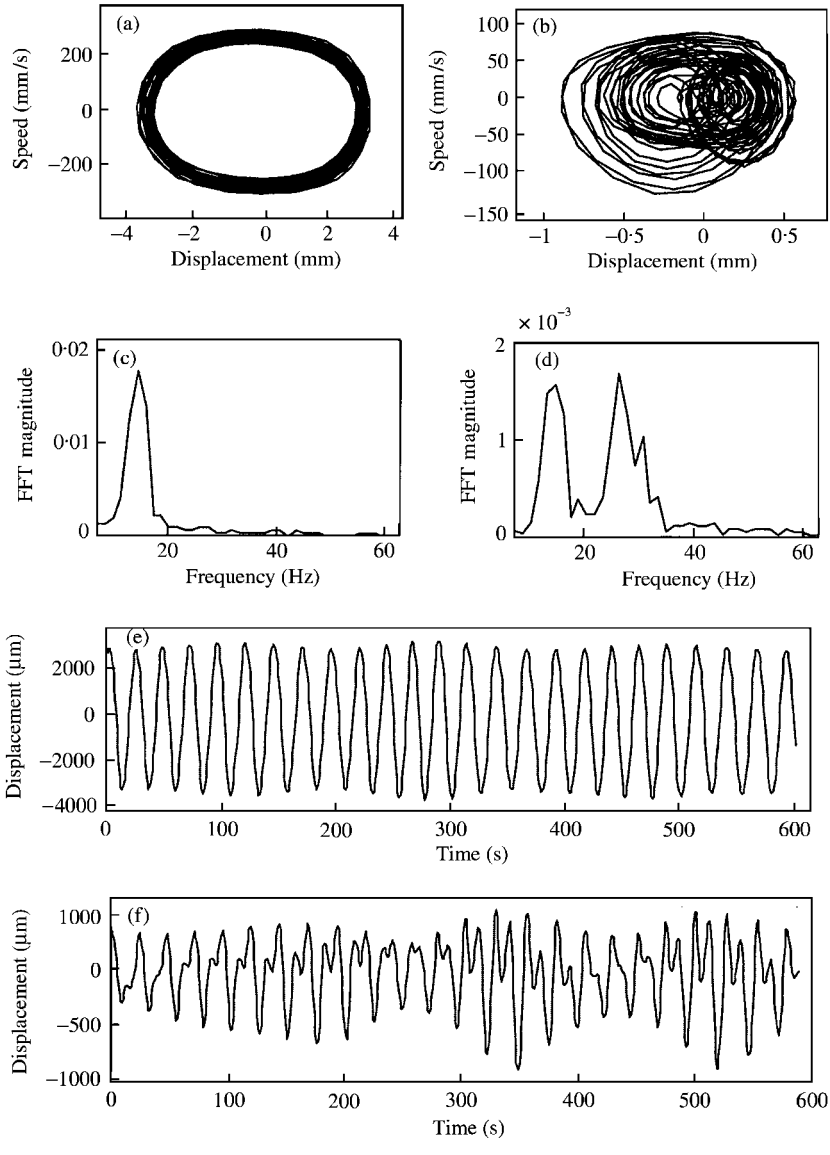

Figure 12. Global simulation results at the frequency excitation of 29·46 Hz. (a) Phase diagram of mode 1; (b) phase diagram of mode 2; (c) FFT of mode 1; (d) FFT of mode 2; (e) temporal response of mode 1; (f) temporal response of mode 2. $W_0 = (0{\cdot}2, 0, 0)$, $\Delta = 0{\cdot}2$, $N_{YO} = 0{\cdot}5$, $N_{YT} = 0{\cdot}2$.

in the response of the plate because the mode of imperfection is exactly the same as the vibration. In the previous case, the fact that the imperfection was in the first mode made the vibration of the plate in the second mode more difficult to obtain. From a practical standpoint, one can say that the interaction between different vibration modes manifests itself in different ways, depending not only on the loading conditions, on the relative positions of the resonance frequencies and on the degree of overlap of their corresponding instability zones as mentioned before [7] but also on the respective nature (symmetric or anti-symmetric) of spatial modes of imperfection and vibration. Because of all these

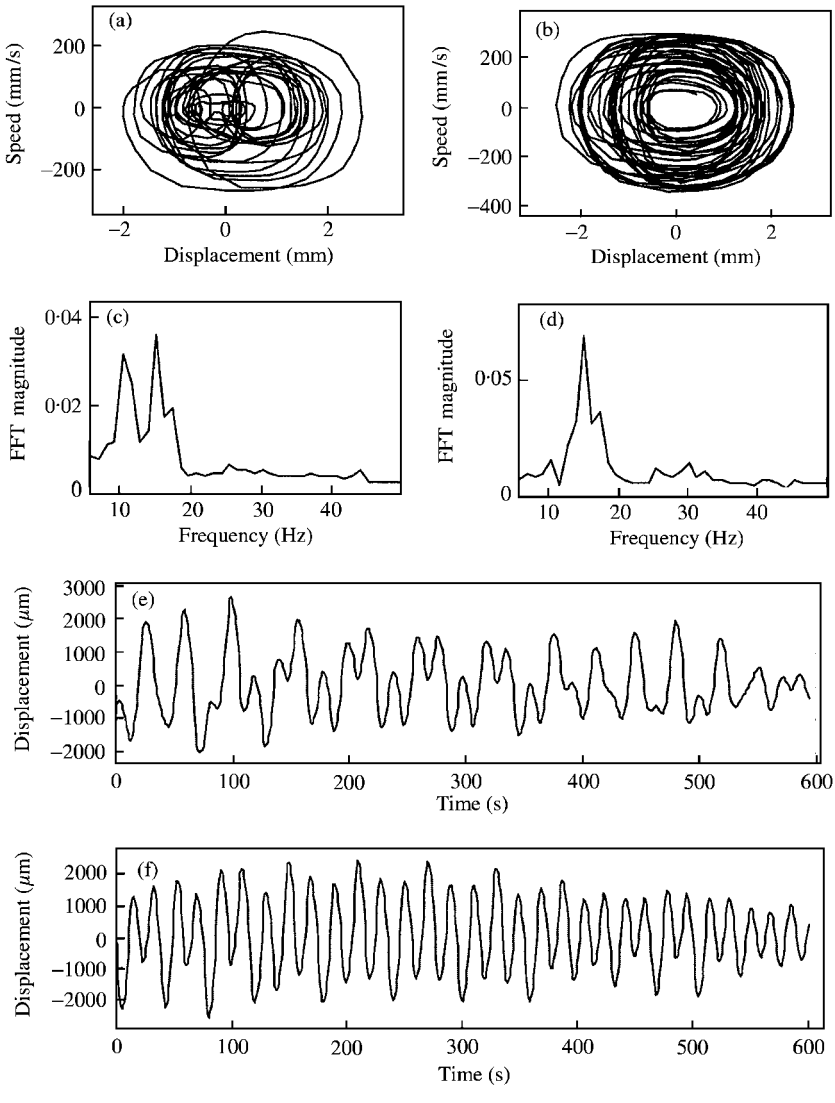

Figure 13. Global simulation results at the frequency excitation of 29·61 Hz. (a) Phase diagram of mode 1; (b) phase diagram of mode 2; (c) FFT of mode 1; (d) FFT of mode 2; (e) temporal response of mode 1; (f) temporal response of mode 2. $W_0 = (0{\cdot}2, 0, 0)$, $\Delta = 0{\cdot}2$, $N_{YO} = 0{\cdot}5$, $N_{YT} = 0{\cdot}2$.

considerations the long-term prediction of the detailed behavior of the system states is impossible unless a numerical simulation like the one presented here is used.

4. CONCLUSIONS

The dynamic response of imperfect plates subjected to in-plane loading has been further investigated using a simulation based on a direct numerical integration procedure. This investigation used new graphical outputs, the temporal response and the phase diagram. It confirmed the previous analytical and numerical results and brought to light some interesting details about modal interaction.

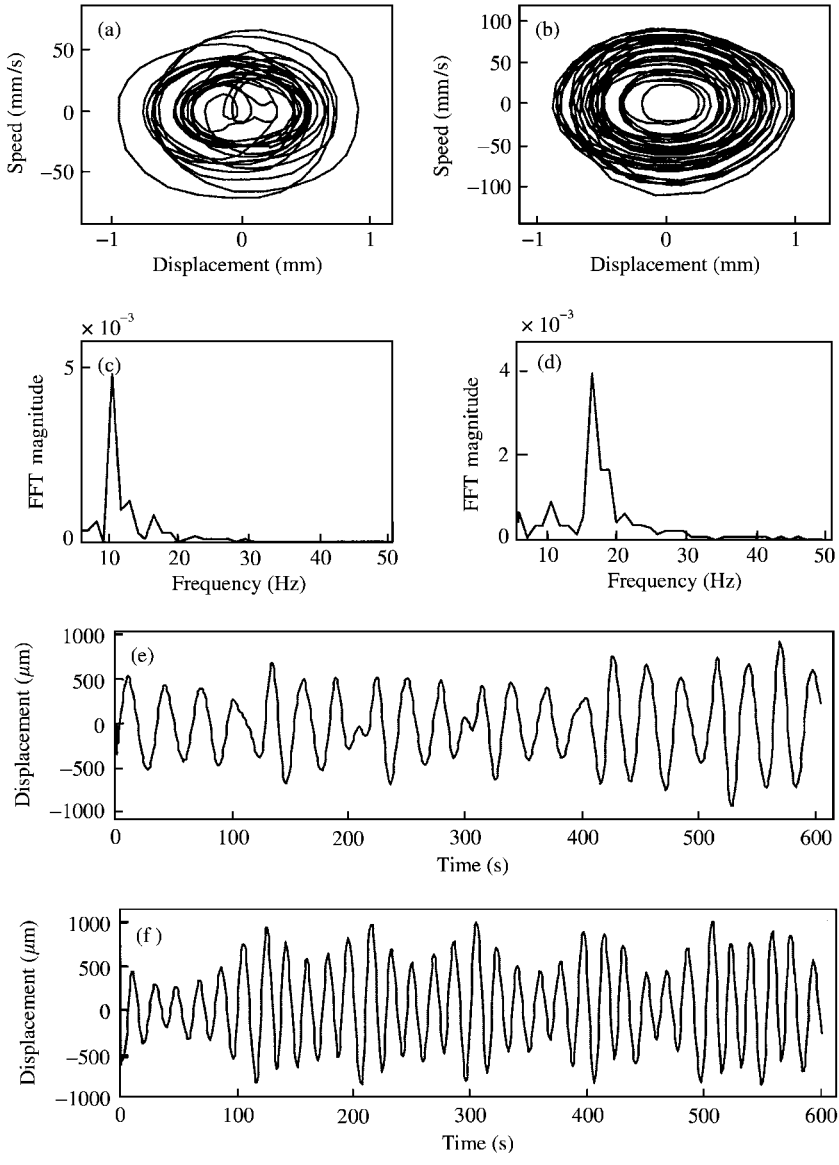

Figure 14. Global simulation results at the frequency excitation of 29·68 Hz. (a) Phase diagram of mode 1; (b) phase diagram of mode 2; (c) FFT of mode 1; (d) FFT of mode 2; (e) temporal response of mode 1; (f) temporal response of mode 2. $W_0 = (0{\cdot}2, 0, 0)$, $\Delta = 0{\cdot}2$, $N_{YO} = 0{\cdot}5$, $N_{YT} = 0{\cdot}2$.

Although the plate dynamic behavior is modelled using a standard differential equation, using a fully deterministic model the resulting motion can have a random nature. The simulation phase diagrams and temporal responses show clearly that the plate can undergo some "unusual or perhaps chaotic" motion in the transition from one kind of resonance to another.

In addition, the simulations have been used to establish the mechanism of interaction between one particular spatial mode of imperfection and the same or a different mode of vibration. It was found that the maximum amplitude of forced vibrations is large when the

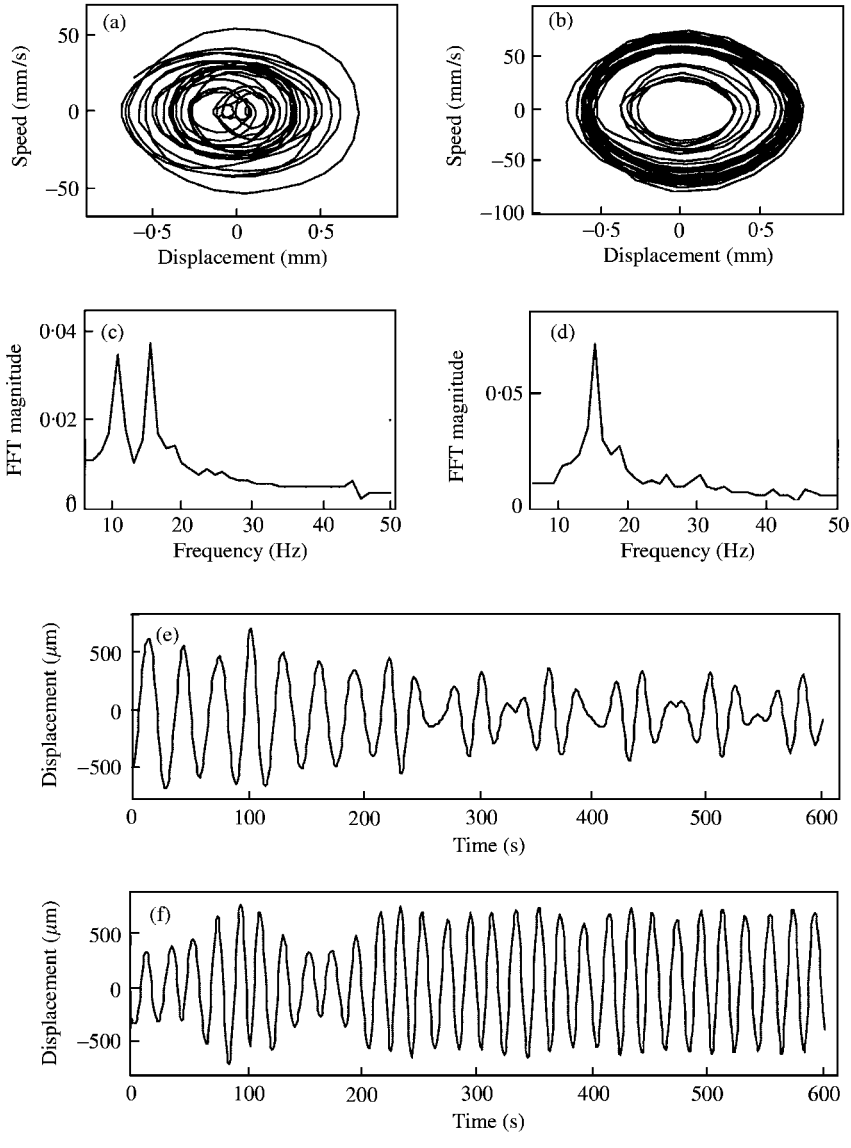

Figure 15. Global simulation results at the frequency excitation of 29·75 Hz. (a) Phase diagram of mode 1; (b) phase diagram of mode 2; (c) FFT of mode 1; (d) FFT of mode 2; (e) temporal response of mode 1; (f) temporal response of mode 2. $W_0 = (0{\cdot}2, 0, 0)$, $\Delta = 0{\cdot}2$, $N_{YO} = 0{\cdot}5$, $N_{YT} = 0{\cdot}2$.

vibration and the imperfection are in the same mode and that the first mode of vibration is always excited whatever the mode of imperfection is.

More generally, this present study has completed the previous ones in demonstrating that the global response of an imperfect plate described by two modes is certainly not the simple superposition of the individual responses of the two modes studied separately. The mechanism of modal interaction was found to be depending not only on the loading conditions, on the relative positions of the resonance frequencies and on the degree of overlap of their corresponding instability zones but also on the nature of the modes (symmetric or anti-symmetric).

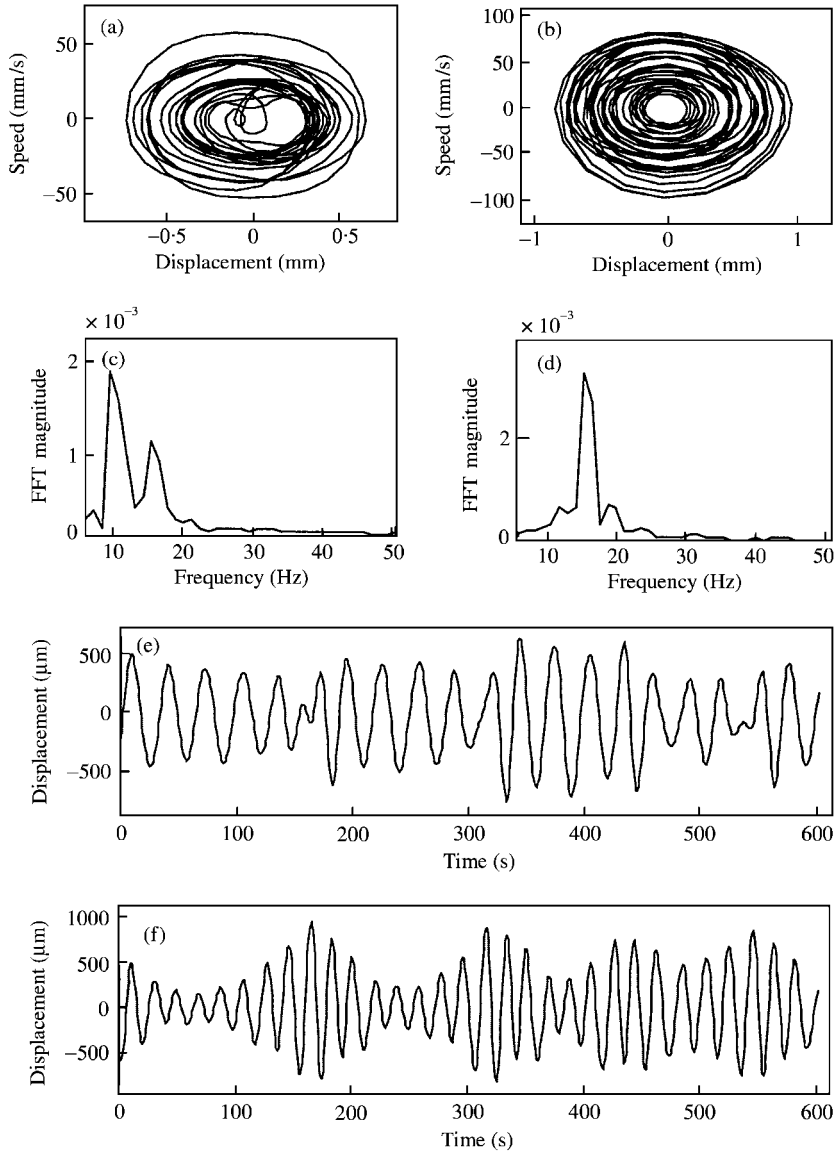

Figure 16. Global simulation results at the frequency excitation of 29·82 Hz. (a) Phase diagram of mode 1; (b) phase diagram of mode 2; (c) FFT of mode 1; (d) FFT of mode 2; (e) temporal response of mode 1; (f) temporal response of mode 2. $W_0 = (0{\cdot}2, 0, 0)$, $\Delta = 0{\cdot}2$, $N_{YO} = 0{\cdot}5$, $N_{YT} = 0{\cdot}2$.

ACKNOWLEDGMENTS

The support of NSERC (the Natural Sciences and Engineering Research Council of Canada) through an individual grant to co-author F. Laville is gratefully acknowledged, as is the contribution of Bechir Hamdaoui for the computer implementation of the model.

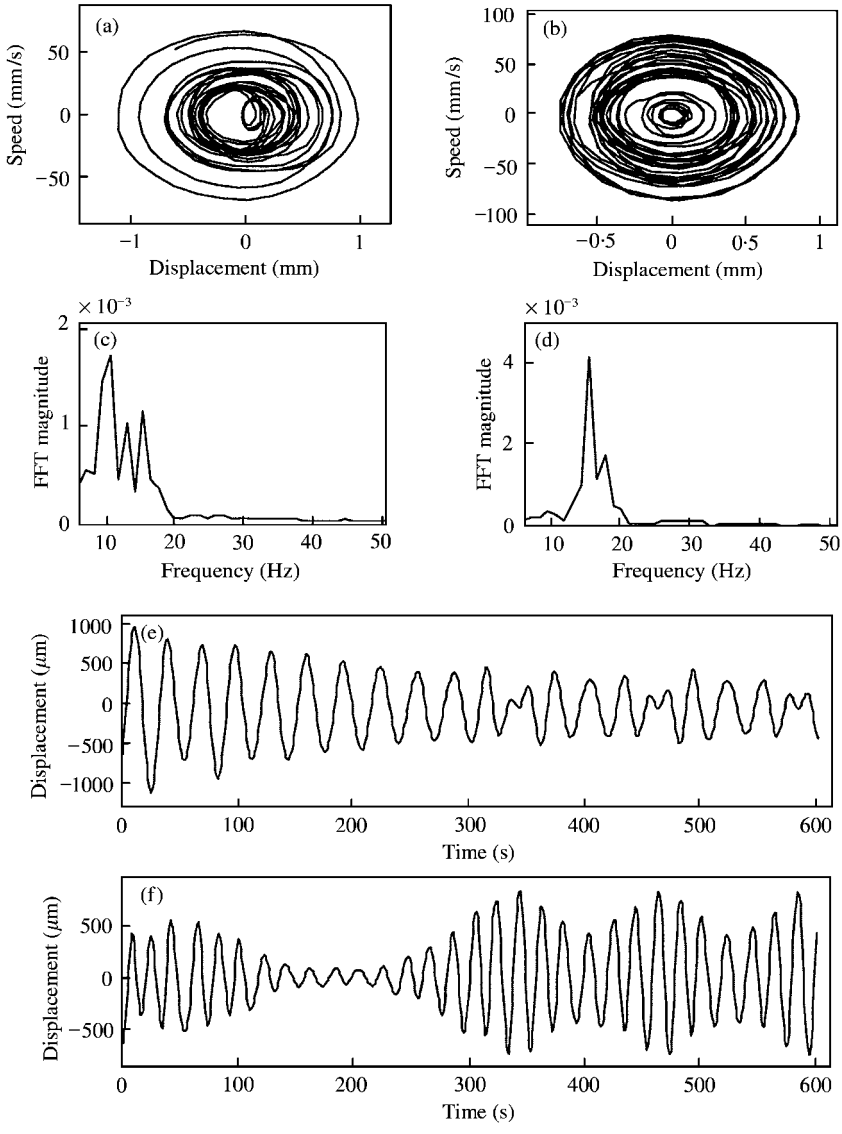

Figure 17. Global simulation results at the frequency excitation of 29·89 Hz. (a) Phase diagram of mode 1; (b) phase diagram of mode 2; (c) FFT of mode 1; (d) FFT of mode 2; (e) temporal response of mode 1; (f) temporal response of mode 2. $W_0 = (0{\cdot}2, 0, 0)$, $\Delta = 0{\cdot}2$, $N_{YO} = 0{\cdot}5$, $N_{YT} = 0{\cdot}2$.

REFERENCES

1. G. L. OSTIGUY 1976 *Ph.D. Dissertation, Syracuse University, Syracuse, New York*. Effects of aspect ratio on parametric response of non-linear rectangular plates.
2. H. NGUYEN 1987 *Ph.D. Dissertation, Ecole Polytechnique de Montréal*. Effects of boundary conditions on the dynamic instability and response of rectangular plates.
3. G. L. OSTIGUY, L. P. SAMSON and H. NGUYEN 1993 *Transactions of the American Society of Mechanical Engineers, Journal of Vibration and Acoustics* **115**, 344–352. On the occurrence of simultaneous resonances in parametrically-excited rectangular plates.

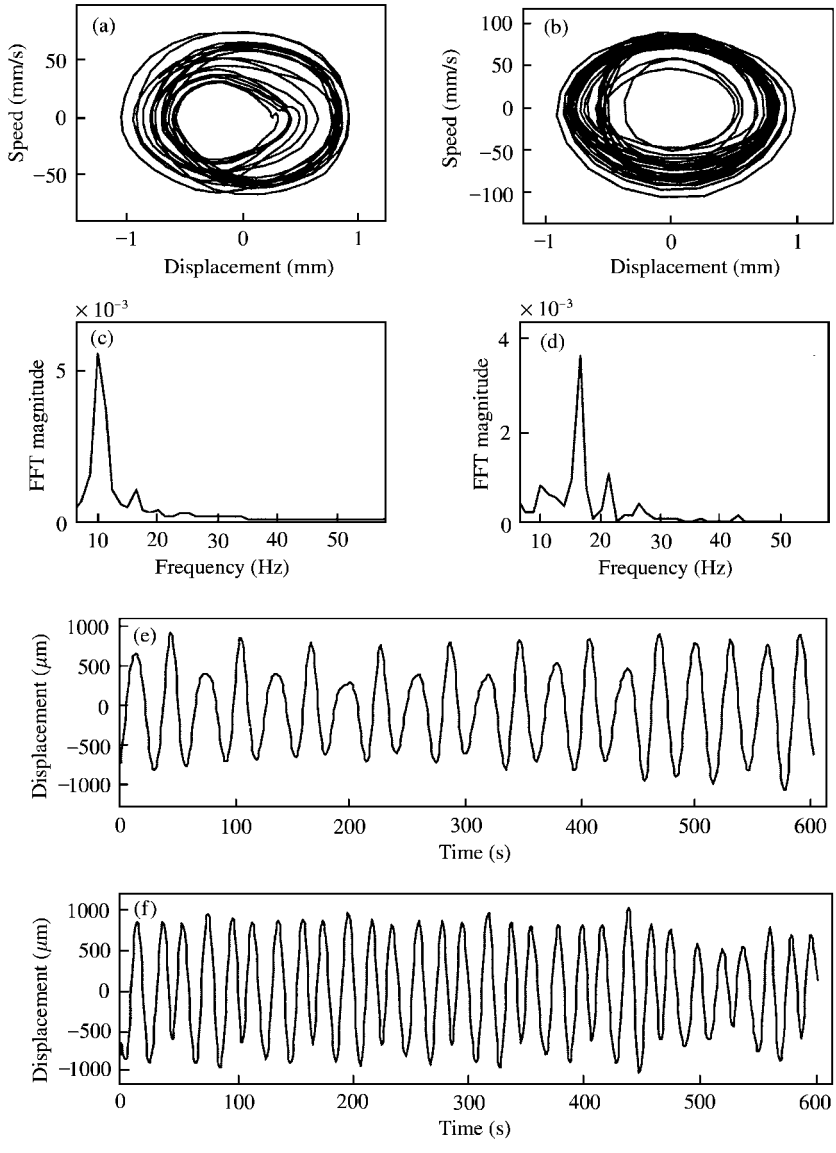

Figure 18. Global simulation results at the frequency excitation of 31·98 Hz. (a) Phase diagram of mode 1; (b) phase diagram of mode 2; (c) FFT of mode 1; (d) FFT of mode 2; (e) temporal response of mode 1; (f) temporal response of mode 2. $W_0 = (0{\cdot}2, 0, 0)$, $\Delta = 0{\cdot}2$, $N_{YO} = 0{\cdot}5$, $N_{YT} = 0{\cdot}2$.

4. S. SASSI and G. L. OSTIGUY 1994 *Journal of Sound and Vibration* **177**, 675–687. Analysis of the variation of frequencies for imperfect rectangular plates.
5. G. L. OSTIGUY and S. SASSI 1992 *Non-linear Dynamics* **3**, 165–181. Effects of initial geometric imperfections on dynamic behavior of rectangular plates.
6. S. SASSI and G. L. OSTIGUY 1994 *Journal of Sound and Vibration* **178**, 41–54. Effects of initial geometric imperfections on the interaction between forced and parametric vibrations.
7. S. SASSI, M. THOMAS and F. LAVILLE 1996 *Journal of Sound and Vibration* **197**, 67–83. Dynamic response obtained by direct numerical integration for pre-deformed rectangular plates subjected to in-plane loading.

8. G. L. OSTIGUY and L. ST-GEORGES 1997 DETC 97 VIB-4186, *American Society of Mechanical Engineers Design Engineering Conference*, September 14–17, Sacramento, California. Dynamic instability and resonances of geometrically imperfect plates.
9. G. L. OSTIGUY, L. ST-GEORGES and S. SASSI 1998 *Transactions of the CSME* **22**, 501–518. Latest developments on the dynamic stability and nonlinear parametric response of geometrically imperfect rectangular plates.